A spatial and seasonal climatology of extreme precipitation return-levels: A case study.

M. Fischer*, U. Ulbrich, H.W. Rust**

Institute of Meteorology, Freie Universität Berlin, Carl-Heinrich-Becker-Weg 6-10, 12165 Berlin

Abstract

A spatial and seasonal modeling approach for precipitation extremes is introduced and exemplified for the Berlin-Brandenburg region in Germany. Monthly maxima of daily precipitation sums are described with a generalized extreme value distribution (GEV) with spatially and seasonally varying parameters. This allows for a return-level prediction also at ungauged sites. The seasonality is captured with harmonic functions, spatial variations are modeled with Legendre polynomials for longitude, latitude and altitude. Interactions between season and space allow for a spatially varying seasonal cycle. Orders of the harmonic and Legendre series are determined using a step-wise forward regression approach with the Bayesian Information Criterion (BIC) as model selection criterion. The longest 80 series are used to verify the approach in a cross-validation experiment based on the Quantile Skill Score (QSS). The model presented describes the observations at all these stations more accurately than a GEV applied to each month and location separately. These improvements are due to the assumption of smoothly varying GEV parameters in time and space; information from neighboring observations in time and space are used to obtain parameters at a given location. Apart from robustness, this approach allows also a seasonally and spatially varying shape parameter and results are found to be more accurate.

Keywords: extreme value statistics, generalized extreme value (GEV) distribution, spatial variation, seasonal variations, extreme precipitation, return-level

*Corresponding author

**Principal corresponding author

Email addresses: madlen.fischer@met.fu-berlin.de (M. Fischer), henning.rust@met.fu-berlin.de (H.W. Rust)

1. Introduction

Severe meteorological events, such as extreme precipitation, severe winter storms or heat waves can lead to considerable damages and might thus have a strong impact on the environment, society and economy (Intergovernmental Panel on Climate Change. Working Group II, 2014, and references therein). Threats due to precipitation are either direct – in form of hail, freezing rain or flash floods – or indirect due to increased erosion, mudslides or river flooding. In particular for the latter the seasonality of extreme precipitation is relevant, since flood risk increases if an increasing probability of extreme precipitation coincides with already high water levels due to, e.g., snow melt (Schindler et al., 2012b,a; Vormoor et al., 2015). In addition, the seasonal cycle of extreme precipitation has a strong impact on crop yields, in particular at early stages of the growing season, the crop is highly vulnerable to damages (Parry et al., 2005; Rosenzweig et al., 2001). Thus, a seasonally resolved risk assessment for extreme precipitation is definitively relevant for certain groups of stakeholders. A risk assessment frequently requires information at ungauged sites, e.g., for insurance companies or for the design of hydraulic structures; spatial information is thus indispensable for a comprehensive risk assessment framework.

To estimate the occurrence probabilities needed for risk assessment, a widely applied concept is extreme value statistics (EVS) (Beirlant et al., 2004; Coles, 2001; Embrechts et al., 1997). Countless applications of EVS have been published in hydrology and climatology (e.g., Lerma et al., 2015; Arns et al., 2015; Brown and Katz, 1995; Coles and Tawn, 1996; Katz et al., 2002; Naveau et al., 2005; Cid et al., 2015; Fischer et al., 2017; Ferreira et al., 2017), to name but a few. One way to address extremes is the block maxima approach. Observations are divided into blocks of equal length and the probability distribution for the maxima of these blocks is described with the generalized extreme value distribution (GEV). Here, we promote a monthly block size contrary to the frequently used annual blocks. However, instead of building a separate extreme value model for each calendar month, we profit from the smooth variation of the maxima's probability distribution across adjacent calendar months. As this variation is intrinsically periodic, the canonical choice is a series of harmonic functions for the GEV parameters, a concept suggested by Rust et al. (2009); Maraun et al. (2009) for the UK. Another advantage of this approach are more accurate return-levels (quantiles) for annual maxima (cf., Fischer et al., 2017). A second choice to model smooth temporal variations are cyclic cubic splines using generalized additive models (Wood, 2006). This approach as been applied by various studies before, e.g. for spatio-temporal climatology of precipitation (Stauffer et al., 2016) or of lightnings (Simon et al., 2017).

Addionally to the generalized additive models, several other approaches of spatial modelling have been established in the extreme value statistics community, e.g., Regional Frequency Analysis (Hosking and Wallis, 2005; Soltyk et al., 2014) where regions of similar statistical characteristics are combined and common probabilities for extremes are obtained, or Bayesian Hierarchical Models (Cooley et al., 2007; Davison et al., 2012) where the spatial variations are taken care of by a large-scale contribution described with linear regression and local variations captured by a spatial stochastic process.

Rust et al. (2013) and Ambrosino et al. (2011) suggest to use spatial coordinates directly as covariates. Instead of expanding the unknown functional relationship between the GEV parameters and the spatial covariates as a Taylor series (i.e. using simple polynomials), they suggest Legendre Polynomials to ensure independence of the terms. In the frame of generalized linear models (GLMs), Rust et al. (2013) and Ambrosino et al. (2011) obtain models for precipitation occurrence (logistic regression) and daily precipitation amounts (Gamma-regression). As this spatial covariates approach is conceptually the same as the seasonal approach in (Rust et al., 2009; Fischer et al., 2017), we combine both in this study.

Additional information of the magnitude and the occurrence probability of extreme precipitation might be beneficial as well. Thus, the goal of this paper is to present a compact and parsimonious spatial-seasonal model which provides monthly resolved return levels at gauged, as well at ungauged sites. This approach is applied to the region of Berlin-Brandenburg as a case study. As data basis, we consider daily precipitation sums for more than 300 rain gauges, presented in Sec. 2. The spatial-seasonal model is based on the GEV for monthly block maxima and is described in Sec. 3. The model selection and validation is covered in Sec. 4 and monthly resolved 100-year return levels are presented in Sec. 5. Finally, we discuss results in Sec. 6.

2. Data

A selection of gauges recording daily precipitation amounts have been obtained from the National Climate Data Center of the German Weather Service (Deutscher Wetterdienst, DWD, `https://werdis.dwd.de/werdis`). Daily precipitation amounts from Hellman rain gauge with a nominal accuracy of 0.1mm are available for almost 5,600 stations. A subset of 322 stations covers the region of Berlin-Brandenburg in the east of Germany (Fig. 1). Some series contain missing observations within the study period. The amount of missing values ranges from several days to several years. We consider the monthly maxima of daily precipitation amounts; months with more than 3 days of missing observations have been excluded from the analysis. In total, our dataset contains 152,401 monthly maxima. For model verification in Sec. 4 we only consider the most complete and longest 80 time series with more than 50 years of observations (blue dots in Fig. 1). The results for the station Berlin-Köpenick (orange triangle) is discussed in more detail.

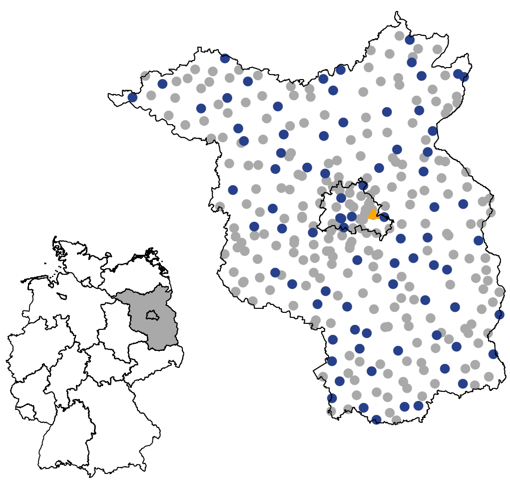

Figure 1: 322 stations in Berlin-Brandenburg (dots) in the east of Germany including 80 long time series with more than 50 years of observations (blue). The example station Berlin-Köpenick is highlighted as a orange triangle.

Furthermore we use geo-referenced altitude from the DIVA-GIS project (`http://www.diva-gis.org/Data`) depicted for Berlin-Brandenburg in Fig. 2.

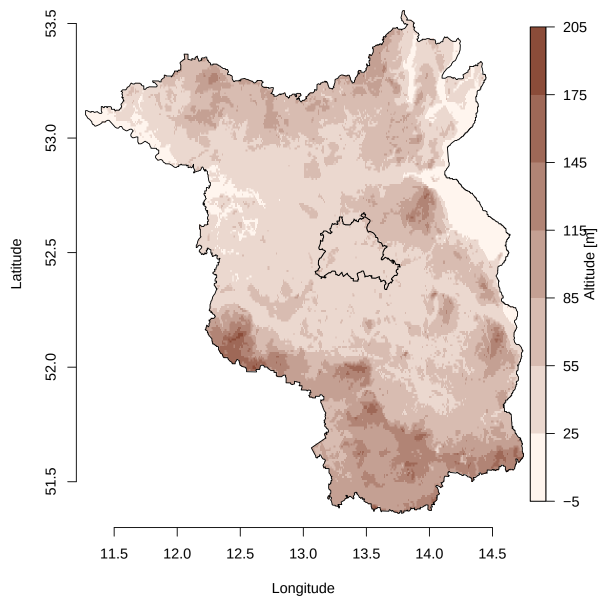

Figure 2: DIVA-GIS geo-referenced altitude with respect to the sea level for Berlin-Brandenburg.

3. Modeling spatial-seasonal extreme precipitation

A statistical description of extremes can be achieved with extreme value statistics (EVS) (Beirlant et al., 2004; Embrechts et al., 1997). This is particularly useful if probabilities of exceeding a given level are to be estimated for the range of observed levels or even beyond. One of the main routes of EVS is the block-maxima approach with the Generalized Extreme Value distribution (GEV) as a model for the probability distribution of maxima from blocks of a certain length, e.g. monthly or annual maxima. Coles (2001) provides a very good introductory text to this topic.

We use a monthly block size and describe the resulting monthly maxima of daily precipitation amounts with the GEV. The GEV parameters are allowed to vary throughout the course of the year and also in space, i.e., with the location of the gauge. This approach follows the idea of linear modeling for the three parameters of the GEV: location, scale and shape. Thus we have basically 3 different sets of linear predictors, one for each parameter. Equation (1) shows the linear predictor for the location parameter μ in a conceptual way:

$$g(\mu) = \mu_0 + f_1(\text{season}) + f_2(\text{space}) + f_3(\text{season}, \text{space}) \tag{1}$$

where g is a link function - for μ the identity function, for σ the logartihm and for ξ the logarithm with an offset of 0.5. Moreover, μ_0 is a constant intercept and f_i are non-linear components represented by linear pre-defined functions. Spatial and seasonal variability are both expanded in terms of adequate basis functions; for the seasonal variations the natural choice are harmonic functions of increasingly higher order described in Sec. 3.2, and for the spatial dimension we chose Legendre polynomials as they form an orthogonal set and thus reduce dependence between terms (Sec. 3.3). The spatial interactions and the dependence to the seasonal variability (f_3) is covered in (Sec. 3.4).

3.1. The block maxima approach

According to the Fisher-Tippett (or Three-Types) Theorem, for independent and identically distributed copies X_i of a random variables X and in the limit of large block-sizes M, the probability distribution for block maxima $Z = \max_i X_i, i = 1, ...M$ converge towards the generalized extreme value distribution (GEV)

$$G(z; \mu, \sigma, \xi) = \exp\left\{ - \left[1 + \xi \left(\frac{z - \mu}{\sigma} \right) \right]^{-1/\xi} \right\} \tag{2}$$

with $\{z : 1 + \xi(z - \mu)/\sigma > 0\}$. The location parameter $-\infty < \mu < \infty$ specifies the position of the probability density function (PDF), the scale parameter $\sigma > 0$ and shape parameter $-\infty < \xi < \infty$ determine the width and shape of the GEV, respectively Coles (2001). This theorem and the generalization for dependent variables (e.g., Leadbetter et al., 1983) provide a strong theoretical background for using the GEV as a model for block maxima.

The block size needed for a sufficiently good approximation with the GEV depends on the nature of the underlying variable and their dependence (Embrechts et al., 1997); the impact on the convergence rate for a few classes of auto-correlated processes is exemplified in Rust (2009). Several studies (Rust et al., 2009; Maraun et al., 2009; Fischer et al., 2017; Schindler et al., 2012a,b) suggest that a monthly block size is suitable for daily precipitation sums at least in the mid-latitudes. Figure 3, showing the monthly Q-Q-plots for the example station Berlin-Köpenick, confirms the choice of a monthly block size for our data set. Monthly maxima can be treaten as independent in time; we also assume independence in space which we justify with the high spatial variability of precipitation compared to the distance of stations. GEV parameters are estimated using iteratively reweighted least squares (IRLS) (Green, 1984) to approximate the maximum-likelihood estimate, as implemented in the package `VGAM` (Yee, 2009) for the environment for statistical computing and graphics `R` (R Core Team, 2014).

Ultimate goal of an EVS analysis is to obtain GEV quantiles for specific probabilities of exceedance, also called the return-levels. The associated return-period $T = 1/(1-p)$ is related to the non-exceedance probability p. Thus, the return-level specifies a magnitude which is expected to be exceeded on average once in a certain time period. In engineering contexts, the 100-year or 1000-year return-level is frequently the basis for dimensioning structures, such as dams or bridges. Asymptotic confidence intervals for return-levels can be derived using the delta method (Coles, 2001).

3.2. Seasonal variations

In the present case, we expect precipitation maxima to vary together with the seasonal cycle. To account for the periodic nature of the seasonality, the time dependence of GEV parameters is described with a series of harmonic functions, e.g., for the location parameter

$$f_1(\text{season}) = \sum_{h=1}^{H} \left[\mu_{h,\sin}\, \sin(h\,\omega\, c_t) + \mu_{h,\cos}\, \cos(h\,\omega\, c_t)\right], \tag{3}$$

with $t = 1, \ldots, 12$ the months in the year, c_t the center of the t-th month given in days starting from January, 1^{st}, $\omega = 2\pi/365.25$ the angular frequency of earth's rotation around the sun and H being the order of the harmonic series expansion (Rust et al., 2009; Maraun et al., 2009; Fischer et al., 2017; Schindler et al., 2012a,b).

3.3. Spatial variations

To capture spatial variations, Ambrosino et al. (2011) and Rust et al. (2013) suggest a series expansion using Legendre polynomials for longitude x, latitude y and altitude z. Legendre polynomials form a set of orthogonal basis functions

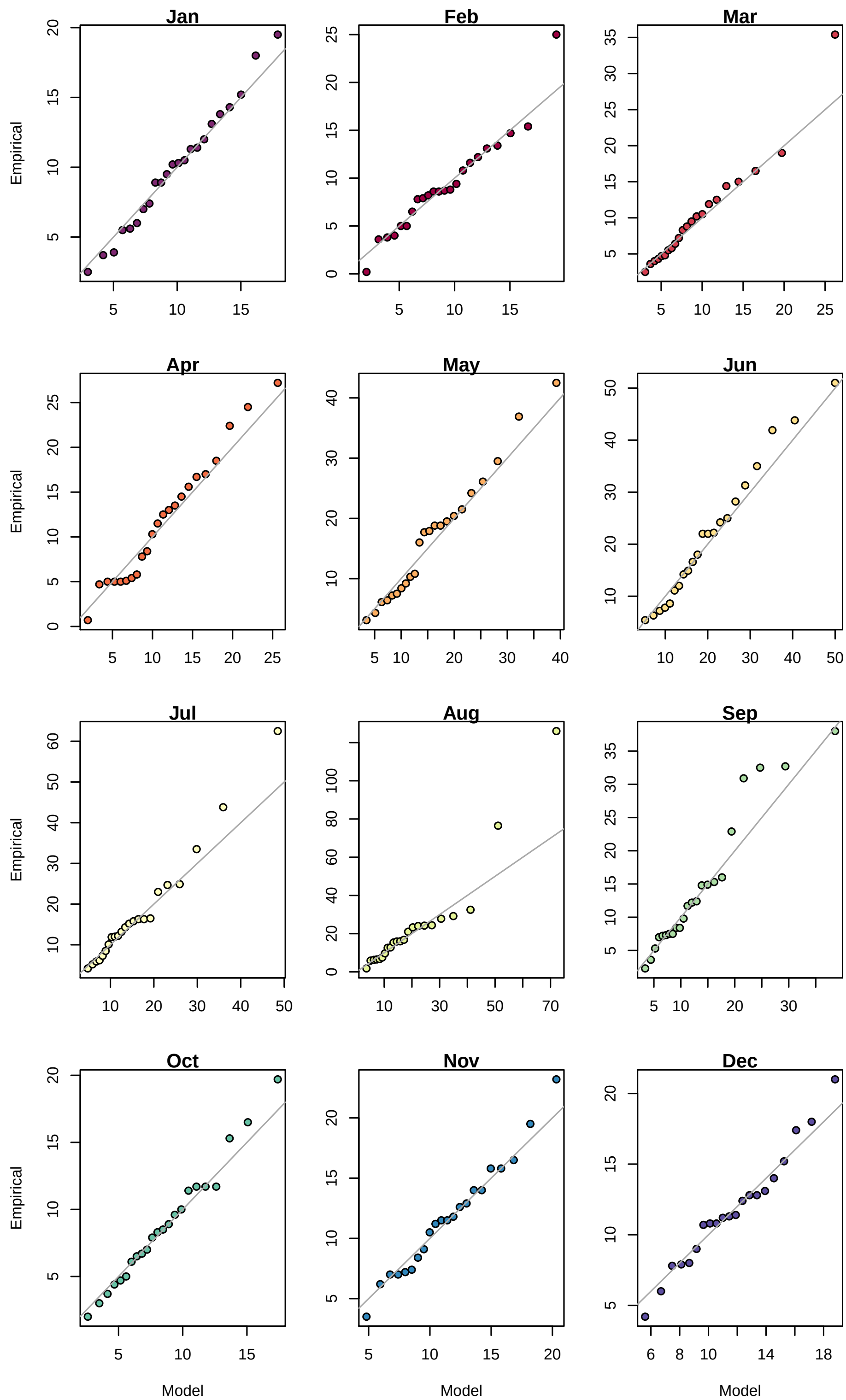

Figure 3: QQ-Plot of all monthly maxima divided into months for the example station Berlin-Köpenick.

on $[-1, 1]$, ensuring linearly independent covariates. We thus obtain as the spatial term in the linear predictor for the location parameter

$$f_2(\text{space}) = \sum_{j=1}^{J} \mu_{j,P} P_j(x) + \sum_{k=1}^{K} \mu_{k,P} P_k(y) + \sum_{l=1}^{L} \mu_{l,P} P_l(z)\,, \tag{4}$$

with $P_j(.)$ denoting the j-th Legendre polynomial which are used for x, y and z, resulting from shifting and scaling longitude, latitude and altitude, respectively. Longitude, latitude and altitude within the cuboid $[-14.8, -11.2] \times [51.3, 53.6] \times [-5, 441]$ (°North $\times$ °East $\times$ m) are shifted and scaled to (x, y, z) such that $(x, y, z) \in [-1, 1] \times [-1, 1] \times [0, 1]$. The maximum altitude of 441 m lies in the south-west of the investigation area shown in Fig. 2, while within the region the highest elevation do not exceed values of 205 m. The spatial term of the predictors for scale and shape are set up analogously.

3.4. Interactions

To allow the seasonal cycle of extreme precipitation to be different in different locations, a spatial variation of the seasonality needs to be accounted for. Within the frame of a GLM, this is realized by so called interaction terms between μ_{season} and μ_{space}. This can be thought of as a model for the spatial variation of the seasonal dependence. In practice, these interactions result as products of the spatial and seasonal covariates. Additionally, dependencies between the different spatial dimensions are integrated as well. Equation (5) gives the interaction for the location parameter μ

$$\begin{aligned}
\mu_{\text{int}} = & \sum_{h_x=1}^{H_{\text{seas,x}}} \sum_{j=1}^{J_{\text{seas,x}}} \left[\mu_{h_x,j,\sin} \sin(h_x\,\omega\,c_t)\,P_j(x) + \mu_{h_x,j,\cos} \cos(h_x\,\omega\,c_t)\,P_j(x)\right] \\
& + \sum_{h_y=1}^{H_{\text{seas,y}}} \sum_{k=1}^{K_{\text{seas,y}}} \left[\mu_{h_y,k,\sin} \sin(h_y\,\omega\,c_t)\,P_k(y) + \mu_{h_y,k,\cos} \cos(h_y\,\omega\,c_t)\,P_k(y)\right] \\
& + \sum_{h_z=1}^{H_{\text{seas,z}}} \sum_{l=1}^{L_{\text{seas,z}}} \left[\mu_{h_z,l,\sin} \sin(h_z\,\omega\,c_t)\,P_l(z) + \mu_{h_z,l,\cos} \cos(h_z\,\omega\,c_t)\,P_l(z)\right] \\
& + \sum_{j_{x,y}=1}^{J_{\text{x,y}}} \sum_{k_{x,y}=1}^{K_{\text{x,y}}} \left[\mu_{j_{x,y},k_{x,y}}\,P_{j_{x,y}}(x)\,P_{k_{x,y}}(y)\right] \\
& + \sum_{j_{x,z}=1}^{J_{\text{x,z}}} \sum_{l_{x,z}=1}^{L_{\text{x,z}}} \left[\mu_{j_{x,z},l_{x,z}}\,P_{j_{x,z}}(x)\,P_{l_{x,z}}(z)\right] \\
& + \sum_{k_{y,z}=1}^{K_{\text{y,z}}} \sum_{l_{y,z}=1}^{L_{\text{y,x}}} \left[\mu_{k_{y,z},l_{y,z}}\,P_{k_{y,z}}(y)\,P_{l_{y,z}}(z)\right]
\end{aligned} \tag{5}$$

Interactions for scale σ and shape ξ are set up analogously.

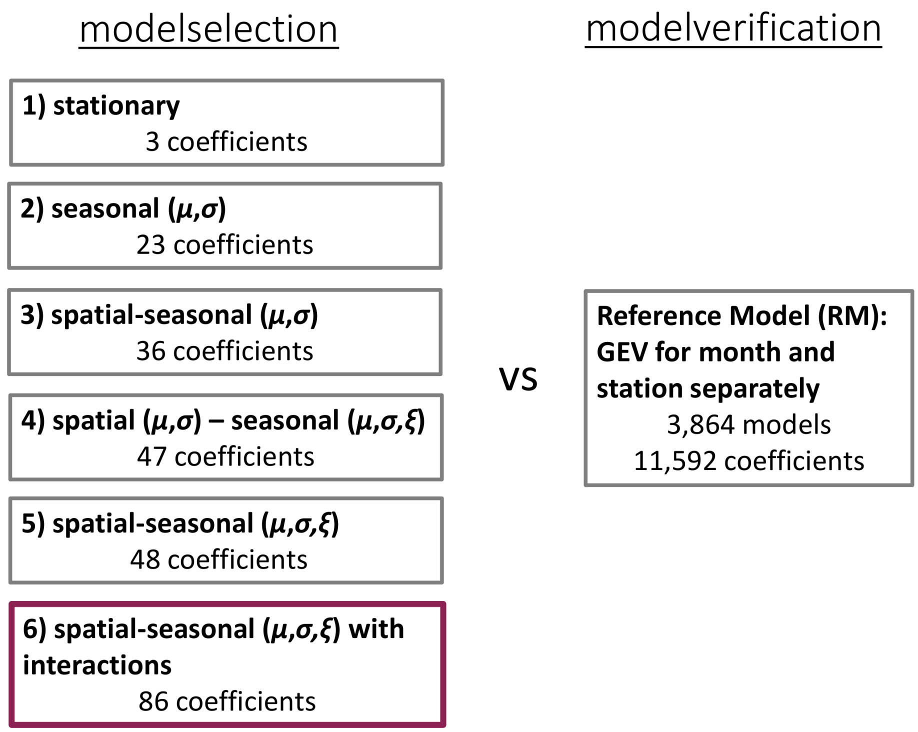

Figure 4: Overview of the model selection steps for monthly maxima of daily precipitation sums (left) and the reference model (right) used for the model verification. The number of coefficients states the amount selected with the BIC.

4. Model building and verification

A spatial-seasonal extreme value model is used to describe the data in the study area. A stationary GEV for monthly maxima at every station with parameters estimated separately for every month of the year is used as a reference model (RM). To analyse the predictors of the final model in detail, different steps of the model selection will be considered: step 1 forms a stationary GEV ingnoring any spatial and seasonal variations. In step 2 the seasonal cycle in location and scale parameter are added using harmonic functions. Subsequently, the spatial variation is included in the predictor for location and scale using Legendre Polynomials of transformed longitude, latitude and altitude, the shape ξ is held constant over space and time (step 3). In the following, we allow for seasonal (step 4) and additionally spatial (step 5) variation of the shape parameter ξ. Finally, interactions between spatial and seasonal terms yield the final step 6. See Fig. 4 for an overview of the different model selection steps and the reference model.

A step-wise forward regression based on the Bayesian Information Criterion (BIC) (Wilks, 2011) is carried out to find the appropriate orders of the harmonic and/or Legendre series expansion. Compared to the RM, the number of parameters in 6) were reduced by a factor of almost 135 to 86. We thus consider model 6) as a successful development if this immense reduction in parameters does not lead to a loss in skill with respect to RM.

4.1. Model building steps

Reference Model (RM). The reference is the canonical stationary GEV with three parameters estimated individually for every month and at every station. This approach leads to 11,592 parameters to estimate: 3 parameters per month at each of the 322 station ($3 \cdot 12 \cdot 322 = 11,592$). The reference model is used for the model verification in Sec. 4.2.

Stationary GEV for all data (1). Starting point of the model selection builds a stationary GEV with three coefficients including all data such that no spatial and temporal variations are considered.

Seasonality in location and scale (2). To describe the variation of the monthly maxima throughout the year a seasonally varying GEV based on harmonic function for location and scale parameter is set up. Higher order harmonics are included subsequently until the BIC is not decreasing anymore. In this setup the whole region is characterized by the same seasonal cycle. Since the shape parameter ξ is difficult to estimate for small datasets, many investigations held this parameter constant (Coles, 2001; Rust et al., 2009; Maraun et al., 2011; Fischer et al., 2017). We will analyse the influence of a seasonal and spatial varying shape parameter in detail in step 4) and 5). For this step the number of preferred coefficients rise up to 23.

Spatial variation in location and scale (3). The seasonal model (2) is straightforwardly extended to a spatial-seasonal model with the BIC as criterion defining the appropriate orders for the Lengendre Polynomials in longitude, latitude and altitude for location and scale. The shape parameter is held constant for the whole study area, yielding a model with 36 coefficients.

Seasonal variation in shape (4). In the following, we aim to give more flexibility to the spatial-seasonal model (3) based on the spatial framework: analogously to the location and scale parameters, the shape parameter ξ is now allowed to vary throughout the year based on a harmonic series. Order selection is again based on the BIC. This leads to 47 coefficients in total.

Spatial variation in shape (5). The subsequent step introduces a spatial component in the shape parameter ξ, analogously to the spatial component in location and scale. Order selection is again based on BIC. The resulting model has 48 coefficients.

order	$\boldsymbol{\mu}$	$\boldsymbol{\sigma}$	$\boldsymbol{\xi}$
H	5	5	5
J	5	1	0
K	4	1	1
L	2	1	0
H_{seas_x} / J_{seas_x}	3/1	4/1	5/1
H_{seas_y} / K_{seas_y}	0/0	3/1	3/1
H_{seas_z} / L_{seas_z}	0/0	0/0	0/0
$J_{x,y}$ / $K_{x,y}$	2/1	0/0	0/0
$J_{x,z}$ / $L_{x,z}$	0/0	0/0	0/0
$K_{y,z}$ / $L_{y,z}$	0/0	0/0	0/0

Table 1: Orders of harmonic series expansion, Legendre Polynomials and interactions for model 5). The orders H refer to Eq. (3), J, K, L to Eq. (4) and H_{int_x} , J_{int_x}, H_{int_y} , K_{int_y}, H_{int_z} , L_{int_z} to Eq. (5)
.

Spatial-seasonal interactions (6). Finally, allowing for interactions between the spatial and seasonal predictors, yields one single model for the study area with 86 coefficients to estimate. The selection of interaction terms is again based on the BIC. Compared to the reference model, we have reduced the number of parameters by a factor of almost 135 to describe the same 152,401 monthly maxima. Tab. 1 provides an overview on selected orders.

Pronounced seasonal variations can be seen for all three parameters of the GEV, while the spatial variations are mainly restricted to the location parameter. Although, a dependence of the seasonal cycle on altitude could be found for Germany (Fischer et al., 2017), the seasonality is here only dependent on the longitude and latitude; the study area has no prominent orography. Furthermore, an interaction between the longitude and latitude is only significant for the location parameter, while the altitude do not show any dependency to the longitude or latitude.

4.2. Verification

To investigate the gain in performance for the individual steps in model building, we use the Quantile Skill Score (QSS) (Bentzien and Friederichs, 2014; Friederichs and Hense, 2007). It is based on the Quantile Score (QS) for the N observations o_n and the p-quantile $z_{p,n}$

$$\mathrm{QS} = \frac{1}{N}\sum_{n=1}^{N}\rho_p(o_n - z_{p,n}) \tag{6}$$

using the so-called check-function ρ_p for $u = o_n - z_{p,n}$

$$\rho_p(u) = \begin{cases} pu & u \geq 0 \\ (p-1)u & u < 0 \end{cases} \tag{7}$$

The Quantile Score is positively oriented and obtains it's optimal value at zero. It extends straightforwardly to the Quantile Skill Score (QSS) for evaluating the performance gain with respect to a reference model

$$\text{QSS} = 1 - \frac{QS_{model}}{QS_{reference}}. \tag{8}$$

Positive/negative values of the QSS indicate a gain/loss in skill with respect to the reference.

As we are interested in the performance gain through the spatial-seasonal modeling approach with respect to the popular station-based approach, we estimate the QSS for models 1) to 6) with RM as the reference, cf. Fig. 4. A robust score is obtained using a block cross-validation procedure (Wilks, 2011). We divide each time series into blocks of three continuous years; each block is used once as validation set. The model is trained in each iteration with the remaining data not falling into the validation set and not into the year before and after it. The QS is then calculated for the associated validation set, the mean QS over all iterations is obtained and the QSS yields the final verification score.

At this point, we only consider the longest 80 stations (blue dots in Fig. 1) for the cross-validation approach. Since the length of the time series differs, the number of cross-validation iterations varies as well. In the steps 1) to 6) we consider the data from all stations for model training except the 5-year block (validation set and year before/after) of the respective time series. For calculating the QS of RM we take the same cross validations sets for the respective stations.

Figure 5 shows the mean cross-validated QSS for the quantiles with p = 0.9, 0.95, 0.99 at each station as dots and the distribution of QSS over all stations as box-whisker plot for the model selection steps 1) to 6). Red values mark locations with a positive QSS, denoting a performance gain with respect to RM. Considering the reference model against the stationary approach for all data (RM vs 1) indicates that spatial and seasonal variations are crucial for describing the observations. Including only the seasonal variations in location and scale parameter does not result in a positive QSS at all stations and considered quantiles (RM vs 2)). Similar, adding the spatial component does not show a considerable performance gain (RM vs 3)). However, the possibility to "borrow strength" from neighboring stations and months allows to model the shape variable in space and throughout the year: a large improvement is obtained by including the seasonality in ξ (RM vs 4)) while adding the spatial component to ξ on top brings only minor changes (RM vs 5)). Adding more flexibility such that different seasonal cycles are allowed at different locations and including dependencies between the spatial dimensions, we end up with a spatial-seasonal model representing the observations at almost all 80 station and for all considered quantiles more accurate than the reference does (RM vs 6)).

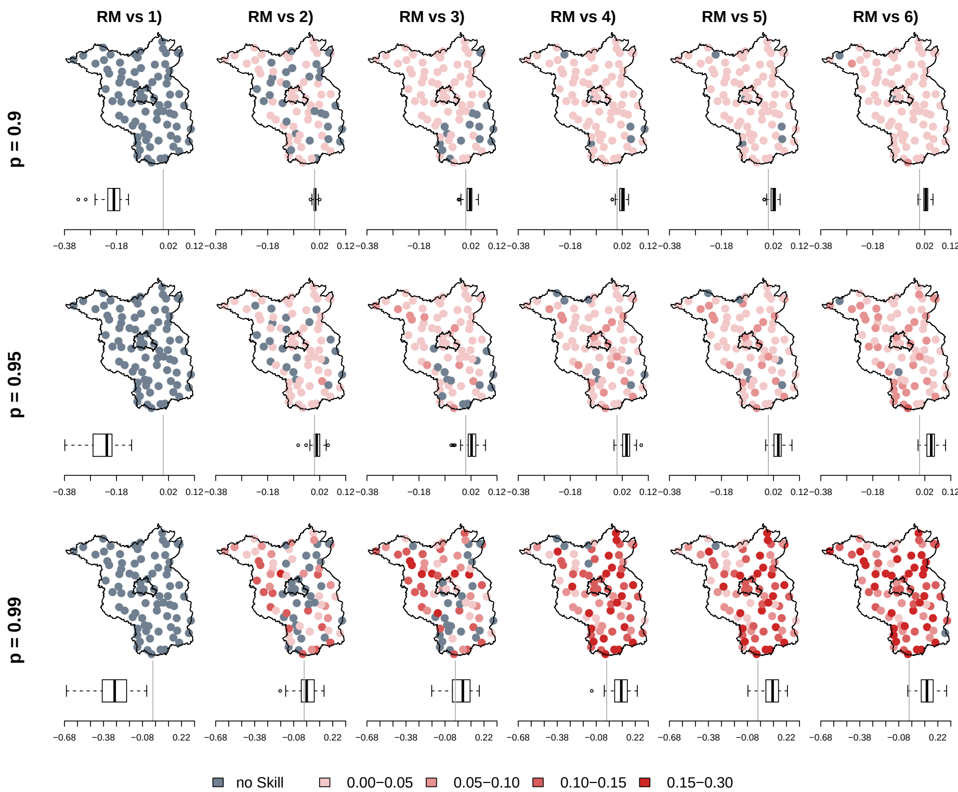

Figure 5: Mean cross-validated QSS for the 80 longest stations for p=0.9,0.95,0.99 (top to bottom line) as colored dots and the whole distribution as box-whisker plot for the steps of the model selection 1) to 6) (from left to right) with reference to RM. Positive values (red) mark an improvement of the model.

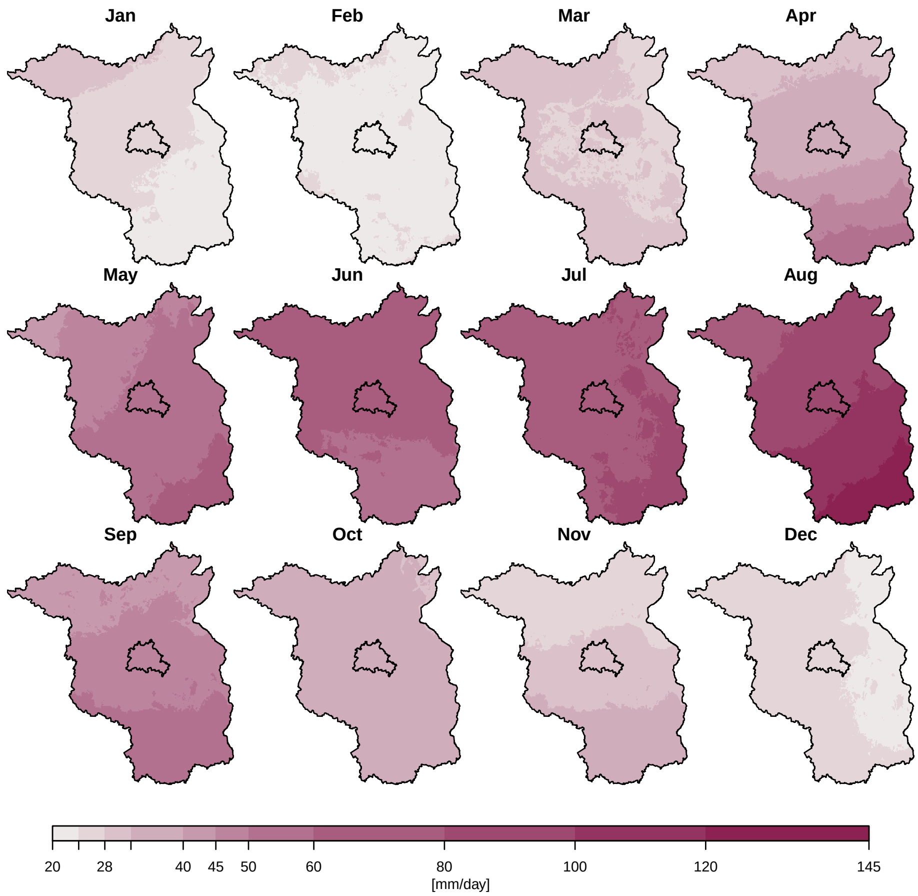

Figure 6: Return level with an annual occurrence probability of 1% (100-year return level) for the center day of each month calculated with the spatial-seasonal model (step 6)).

5. Spatial-seasonal return levels

Since the 100-year return level is typically of particular interest in risk assessment and infrastructure planning, Fig. 6 maps this quantity for the study area for each month of the year. A pronounced seasonal cycle is visible with 100-year return levels lower than 32 mm/day in the winter month and more than 120 mm/day in the southern part in summer. We interpret this as a sign of convective precipitation events dominating in summer. We will analyse this in further investigations.

Figure 7 shows the monthly maxima of daily precipitation sums for the example station Berlin-Köpenick (observation period: 1969-01-01 to 1995-12-31) as Box-Whisker-Plot (Grey) with the empirical 0.99-quantile marked as a horizontal black line for each month. Additionally, the four panels show return level estimates for non-exceeding probabilities $p = 0.25$, $p = 0.5$, $p = 0.75$, and $p = 0.99$ as colored solid lines from bottom to top obtained from the reference model (a), and the subsequent model building 1), 2) and 4) (b-d). For the 1st to 3rd quartile ($p = 0.25$, $p = 0.5$ and $p = 0.75$) the three model setups all agree quite well with the empirical quantiles, although slight differences exist. Discrepancies are more readily visible for larger quantiles, e.g. for the 0.99-quantile (100-year return levels, blue solid lines) in Fig. 7. As already discussed in Sec. 4.2, the model of step 1) (panel b), which excludes all spatial and temporal variations, can not represent the observations sufficiently. The levels obtained from the reference model are in general higher, particularly the peak in August cannot be reproduced very well by step 2) (panel c). The rigidity of the "seasonal only"-model, particularly the constant shape throughout the year, is responsible for the very smooth and moderate 0.99-quantile; the single shape parameter in the seasonal model characterizes extremes for all months, whereas in the more flexible RM each month is associated with an individual shape parameter. As particularly the shape parameter is difficult to estimate, uncertainty is large in the RM and it bears the risk of over-parameterization. On the contrary, the model of step 2) is likely to be too rigid as it is not able to capture the strong extremes in with a shape parameter being constant throughout the year and thus not able to account for different characteristics of winter and summer events with different precipitation mechanisms dominating. The model of step 2) does show a peak in the 0.99-quantile in August but much smaller than in RM. The results of step 2) and step 4) indicates that a seasonal variation of the shape parameter seems to be necessary for the situation at hand with dominating precipitation mechanisms varying throughout the year. This is then realized in the spatial-seasonal framework (steps 4) to 6)). The quantiles selected for presentation do not differ visually between these three models (4) to 6)). Panel (d) in Fig. 7 shows that the spatial-seasonal model including interactions (model 6)) leads to a relatively smooth seasonal cycle which is, however, able to reflect the large summer extremes and the lower winter events.

The 0.99-quantile is strongly influenced by the shape parameter, depicted in Fig. 8 for all months calculated with the RM (black) and the final spatial-seasonal model (blue). The differences of the shape parameters are very pronounced, as the seasonal smoothness for the spatial-seasonal model does not allow such a strong deviation for only one month. In addition, Fig. 8 illustrates the general characteristic of the seasonal precipitation: in the winter month the shape parameter is around zero or even negative, resulting in return levels with an upper bound, while in summer the shape parameter reaches exclusively positive values leading to a distribution with more extreme events.

Uncertainties of the return levels can be quantified using the asymptotic approximation and the delta method (Coles, 2001). For the models shown in Fig. 7 (a) and (b), the 95% uncertainty intervals are to large to display, in particular for the 100-year return levels.

Figure 9 shows the logarithm of the variance of the 100-year return level for Berlin-Köpenick colored for the different months. It can be seen, that the uncertainties of the reference model (RM) and all model selection steps are in

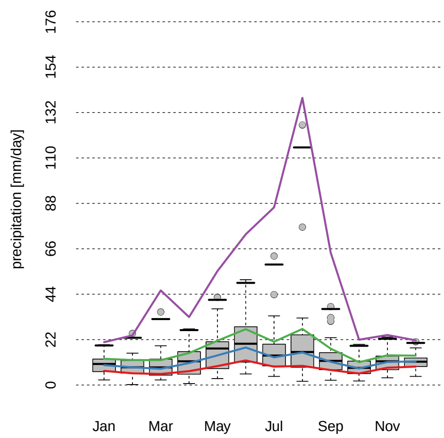

(a) RM

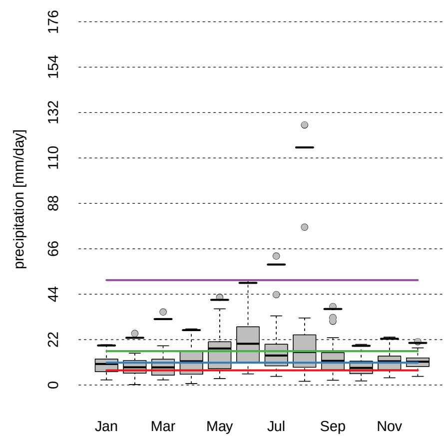

(b) Step 1

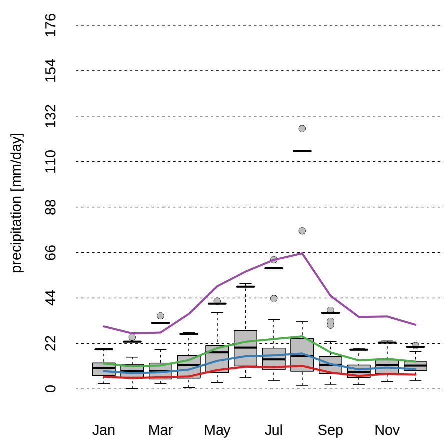

(c) Step 2

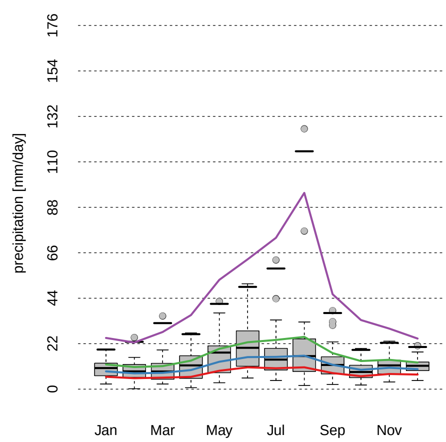

(d) Step 4

Figure 7: Monthly maxima of daily precipitation sums of the Station Berlin-Köpenick (1969-01-01 to 1995-12-31) as Box-Whisker Plot (Grey) with the median as black line within the box, first and third quartile as box boundaries, the whiskers extend to the maxima/minima but measure at most the 1.5 inter-quartile range, data points outside the whiskers are plotted as open circles. Additionally, the empirical 0.99-quantiles are plotted as horizontal lines. To each panel Return levels are added as solid lines for $p = 0.25$ (red), $p = 0.5$ (blue), $p = 0.75$ (green) and $p = 0.99$ (violet) obtained from the reference model (a) and the model building steps 1),2) and 4) (b-d). The results of step 3) do not differ visually from step 2) and step 5) and 6) are similar to step 4).

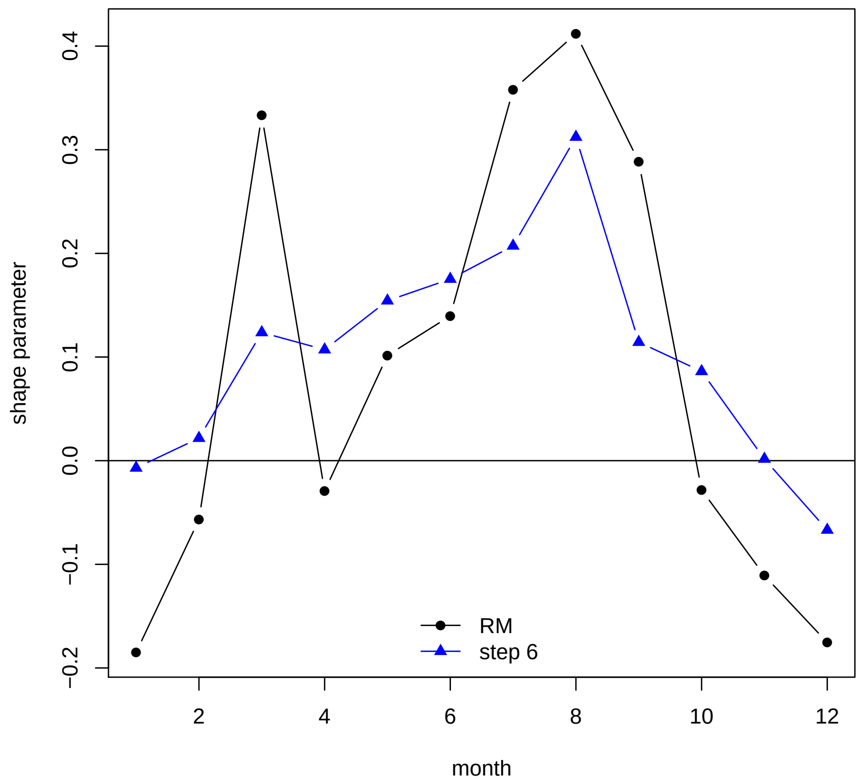

Figure 8: Shape parameter for the reference model (RM, black) and the final spatial-seasonal model (step 6), blue).

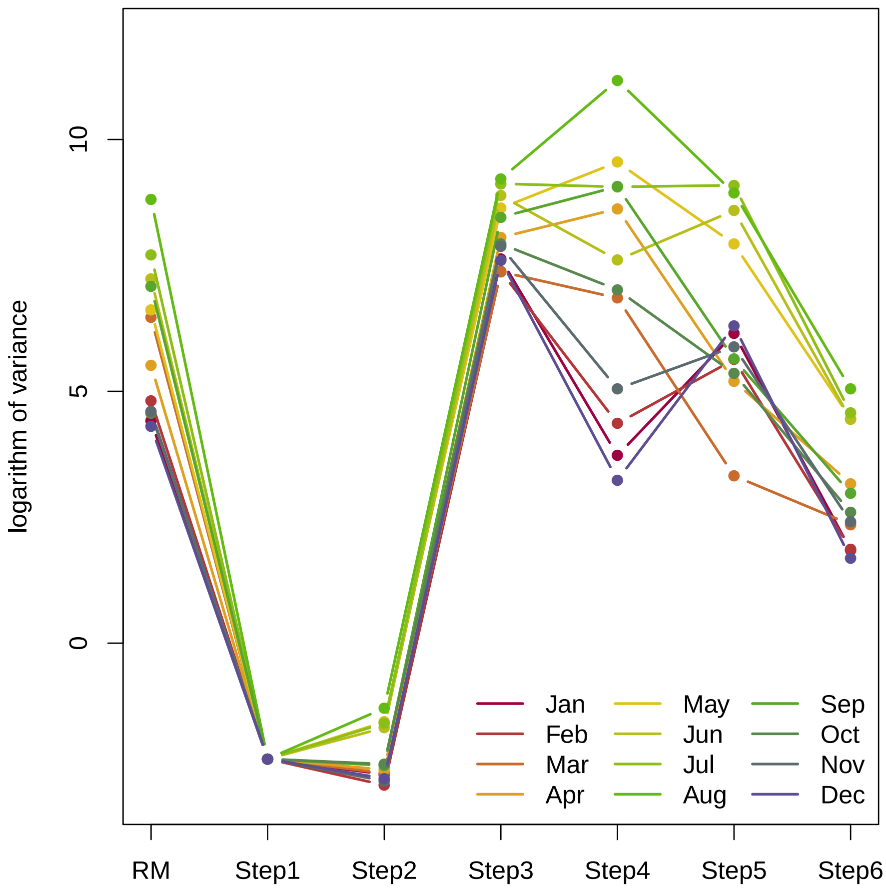

Figure 9: Logarithm of the variance of the 100-year return level for the example station Berlin-Köpenick for the reference model (RM) and the models 1) to 5) for all months of the year.

general lower in winter than in summer. Due to the small number of coefficients and a comparably large number of data points for modeling steps 1) and 2), the variance is low compared to other modeling steps with more coefficients. Due to the lack of skill (Fig. 5) and the lack of spatial information those modeling steps are not favourable here. Steps 3) to 5) partly result in higher uncertainties than the reference model, probably due to the lower flexibility of those models. While the seasonal modeling in μ and σ (step 2) lead to a gain only in the summer month, the seasonal variation of the shape parameter (step 4) is important for the winter month. The spatial variations only (models 3 and 5) do not lead to smaller variances for the return levels. It can be seen, that the interaction terms are necessary: the final spatial-seasonal model (step 6) provides the lowest uncertainties in all months.

6. Conclusion

We describe monthly precipitation maxima of 322 stations in Berlin-Brandenburg with a spatial-seasonal extreme value model based on the Generalized Extreme Value distribution (GEV) with parameters depending on space and season. The seasonal variations in the parameters are captured with a series of harmonic functions and their spatial variations with Legendre Polynomials for longitude, latitude and altitude. Furthermore, we add interactions between seasonal and spatial predictors as well as for the different spatial dimensions. Order selection for the harmonic series and the Legendre polynomials is based on the Bayesian Information Criterion (BIC) in the frame of a step-wise forward regression. The reference for the model verification is a stationary GEV describing monthly maxima separately for every month of the year and for every station. Starting point of the model selection builts a stationary approach for all data such that no variation in time and space are included. In a next step seasonal variations for location and scale parameter are considered. This is augmented in a third step towards a spatial-seasonal model for location and scale parameter, the shape parameter is held constant. As the framework of one spatial-seasonal model for all stations allows to "borrow strength" for parameter estimation from the neighboring stations and months, we allow in the following steps the shape parameter to vary throughout the year (model 4) and additionally in space (model 5). Finally, interactions between seasonal and spatial predictors and spatial dimensions are included, i.e. the seasonal dependence is now allowed to vary in space. This final model uses 86 parameters to describe more than 150,000 monthly maxima. Compared to the canonical 3-parameter GEV for every station and month, this is a reduction in parameters by a factor of almost 135.

The intermediate steps and the final model 6) are compared in a forecast verification setting against the reference model using block-cross-validation with the Quantile Skill Score (QSS) for the longest 80 time series. The stationary model (step 1) shows a negative skill for all stations, and the seasonal-only model (step 2), as well as the spatial-seasonal model (step 3) for a number of stations. A considerable improvement in skill comes with the possibility of a seasonally varying shape parameter in the spatial-seasonal models (step 4, 5 and 6). The spatial-seasonal model with interactions finally leads to positive skill at all 80 stations considered for verification.

Additionally, we show a map of monthly 100-year return levels for Berlin-Brandenburg and thus return-level information at ungauged sites derived from the final spatial-seasonal model. The region is characterized by a very pronounced seasonal cycle with lower return levels in winter and higher levels in summer; likely a result of convection being the dominating mechanism for extreme precipitation in summer, but not in winter. This results in particular attention to the management of fire brigade operations in summer months (e.g. pumping-out of flooded basements, rescue and evacuation) or for protection of growing plants.

The station Berlin-Köpenick is used to illustrate the effects of the different steps in the model building procedure with a focus on the 100-year return level. The reference model allows for individual shape parameters for each month and shows levels considerably larger in summer than in winter, pointing towards the need of a seasonal shape parameter. As the models 2) and 3) do not allow for seasonality in the shape, they cannot account for the observed seasonal changes in extreme precipitation characteristics. Only models 4) to 6) with a seasonally varying shape are able to capture this effect. Compared to the reference, a dramatic reduction in the number of parameters (factor 135) can be achieved with model 6), accompanied by a 10% gain skill in performance (for the 0.99 quantile) and a reduction in uncertainty.

The presented strategy does not account for influences on extreme precipitation, for example orographic lifting is only partially captured by including altitude. Thus a transfer of this approach to regions with strong orographic variations might not be appropriate. In those regions, a modeling approach might profit from the inclusion of predictors accounting for the orography-induced mechanisms. Other approaches for spatial extreme value modeling might also perform well, e.g. Bayesian Hierarchical Models (BHM) (i.e. Cooley et al., 2007; Davison et al., 2012) or Generalized Additive Models (GAM) implemented in R for example in the mgcv package (Wood, 2017). .

We consider the approach presented as a highly valuable extension to risk assessment. The advantages over conventional stationary (single-station, single months) extreme value models are: straightforward extension of conventional GEV modeling with covariates, information at ungauged sites, dramatically less parameters to be estimated, reduced uncertainty and improved performance.

Acknowledgments

This study has been partially funded by the Deutsche Forschungsgemeinschaft (DFG) within the research training programme *NatRiskChange* GRK 2043/1 at Potsdam University and partially by Deutsche Forschungsgemeinschaft (DFG) through grant CRC 1114 "Scaling Cascades in Complex Systems", Project A01 “Coupling a multiscale stochastic precipitation model to large scale atmospheric flow dynamics”. HWR acknowledges support by the Freie Universität Berlin within the Excellence Initiative of the German Research Foundation. Additionally, the authors thank the National Climate Data Center of the German Weather Service (DWD) for providing and maintaining the precipitation datasets via the online portal WebWerdis (`https://werdis.dwd.de`). The analysis was carried out using `R`, an environment for statistical computing and graphics (Team, 2016), based on the `VGAM` package (Yee, 2015).

References

Ambrosino, C., Chandler, R. E., Todd, M. C., 2011. Southern african monthly rainfall variability: An analysis based on generalized linear models. Journal of climate 24 (17), 4600–4617.

Arns, A., Wahl, T., Haigh, I. D., Jensen, J., 2015. Determining return water levels at ungauged coastal sites: a case study for northern germany. Ocean Dynamics 65 (4), 539–554.

Beirlant, J., Goegebeur, Y., Segers, H., Teugels, J., 2004. Statistics of Extremes: Theory and Applications. Series in Probability and Statistics. Wiley.

Bentzien, S., Friederichs, P., 2014. Decomposition and graphical portrayal of the quantile score. Quarterly Journal of the Royal Meteorological Society 140 (683), 1924–1934.

Brown, B. G., Katz, R. W., 1995. Regional analysis of temperature extremes: spatial analog for climate change? Journal of Climate 8 (1), 108–119.

Cid, A., Menéndez, M., Castanedo, S., Abascal, A. J., Méndez, F. J., Medina, R., 2015. Long-term changes in the frequency, intensity and duration of extreme storm surge events in southern europe. Climate Dynamics, 1–14.

Coles, S. G., 2001. An Introduction to Statistical Modelling of Extreme Values. Springer, London.

Coles, S. G., Tawn, J. A., 1996. A Bayesian analysis of extreme rainfall data. Appl. Stat. 45, 463–478.

Cooley, D., Nychka, D., Naveau, P., 2007. Bayesian spatial modeling of extreme precipitation return levels. Journal of the American Statistical Association 102 (479), 824–840.

Davison, A. C., Padoan, S., Ribatet, M., 2012. Statistical modeling of spatial extremes. Statistical Science, 161–186.

Embrechts, P., Klüppelberger, C., Mikosch, T., 1997. Modelling Extremal Events for Insurance and Fincance. Springer, Berlin.

Ferreira, A., Friederichs, P., de Haan, L., Neves, C., Schlather, M., 2017. Estimating space-time trend and dependence of heavy rainfall. arXiv preprint arXiv:1707.04434.

Fischer, M., Rust, H. W., Ulbrich, U., 2017. Seasonality in extreme precipitation– using extreme value statistics to describe the annual cycle in german daily precipitation extreme. Meteorologische Zeitschrift, accepted.

Friederichs, P., Hense, A., 2007. Statistical downscaling of extreme precipitation events using censored quantile regression. Monthly weather review 135 (6), 2365–2378.

Green, P. J., 1984. Iteratively reweighted least squares for maximum likelihood estimation, and some robust and resistant alternatives. Journal of the Royal Statistical Society. Series B (Methodological), 149–192.

Hosking, J. R. M., Wallis, J. R., 2005. Regional frequency analysis: an approach based on L-moments. Cambridge University Press.

Intergovernmental Panel on Climate Change. Working Group II, 2014. Climate Change 2014: Impacts, Adaptation, and Vulnerability.

Katz, R. W., Parlange, M. B., Naveau, P., 2002. Statistics of extremes in hydrology. Advances in Water Resources 25, 1287–1304.

Leadbetter, M. R., Lindgren, G., Rootzén, H., 1983. Extremes and related properties of random sequences and processes. Springer Series in Statistics. Springer, New York.

Lerma, A. N., Bulteau, T., Lecacheux, S., Idier, D., 2015. Spatial variability of extreme wave height along the atlantic and channel french coast. Ocean Engineering 97, 175–185.

Maraun, D., Rust, H. W., Osborn, T. J., 2009. The annual cycle of heavy precipitation across the UK: a model based on extreme value statistics. J. Climatol. 29 (12), 1731–1744.

Maraun, D., Rust, H. W., Osborn, T. J., 2011. The influence of synoptic airflow on UK daily precipitation extremes. Part I: observed spatio-temporal relations. Clim. Dyn. 36 (1-2), 261–275.

Naveau, P., Nogaj, M., Ammann, C., Yiou, P., Cooley, D., Jomelli, V., 2005. Statistical methods for the analysis of climate extremes. C.R. Geoscience 377, 1013–1022.

Parry, M., Rosenzweig, C., Livermore, M., 2005. Climate change, global food supply and risk of hunger. Philosophical Transactions of the Royal Society of London B: Biological Sciences 360 (1463), 2125–2138.

R Core Team, 2014. R: A language and environment for statistical computing. r foundation for statistical computing, vienna, austria, 2012.

Rosenzweig, C., Iglesias, A., Yang, X., Epstein, P. R., Chivian, E., 2001. Climate change and extreme weather events; implications for food production, plant diseases, and pests. Global change & human health 2 (2), 90–104.

Rust, H. W., 2009. The effect of long-range dependence on modelling extremes with the generalised extreme value distribution. Europ. Phys. J. Special Topics 174, 91–97.

Rust, H. W., Maraun, D., Osborn, T. J., 2009. Modelling seasonality in extreme rainfall: a UK case study. Europ. Phys. J. Special Topics 174, 99–111.

Rust, H. W., Vrac, M., Sultan, B., Lengaigne, M., Jun. 2013. Mapping weather-type influence on senegal precipitation based on a spatial-temporal statistical model. J. Climate 26, 8189–8209.
URL http://dx.doi.org/10.1175/JCLI-D-12-00302.1

Schindler, A., Maraun, D., Luterbacher, J., 2012a. Validation of the present day annual cycle in heavy precipitation over the british islands simulated by 14 rcms. Journal of Geophysical Research: Atmospheres (1984–2012) 117 (D18).

Schindler, A., Maraun, D., Toreti, A., Luterbacher, J., 2012b. Changes in the annual cycle of heavy precipitation across the british isles within the 21st century. Environmental Research Letters 7 (4), 044029.

Simon, T., Umlauf, N., Zeileis, A., Mayr, G. J., Schulz, W., Diendorfer, G., 2017. Spatio-temporal modelling of lightning climatologies for complex terrain. Natural Hazards and Earth System Sciences 17 (3), 305.

Soltyk, S., Leonard, M., Phatak, A., Lehmann, E., et al., 2014. Statistical modelling of rainfall intensity-frequency-duration curves using regional frequency analysis and bayesian hierarchical modelling. In: Hydrology and Water Resources Symposium 2014. Engineers Australia, p. 302.

Stauffer, R., Mayr, G. J., Messner, J. W., Umlauf, N., Zeileis, A., 2016. Spatio-temporal precipitation climatology over complex terrain using a censored additive regression model. International Journal of Climatology.

Team, R. C., 2016. R: A language and environment for statistical computing. vienna: R foundation for statistical computing; 2014.

Vormoor, K., Lawrence, D., Heistermann, M., Bronstert, A., 2015. Climate change impacts on the seasonality and generation processes of floods–projections and uncertainties for catchments with mixed snowmelt/rainfall regimes. Hydrology and Earth System Sciences 19 (2), 913–931.

Wilks, D. S., 2011. Statistical methods in the atmospheric sciences. Vol. 100. Academic press.

Wood, S., 2006. Generalized additive models: an introduction with R. CRC press.

Wood, S., 2017. Generalized Additive Models: An Introduction with R, 2nd Edition. Chapman and Hall/CRC.

Yee, T. W., 2009. VGAM: Vector Generalized Linear and Additive Models. R package version 0.7-9.
URL http://CRAN.R-project.org/package=VGAM

Yee, T. W., 2015. Vector Generalized Linear and Additive Models: With an Implementation in R. Springer, New York, USA.